

# In<sup>III</sup>-Catalysed Tandem C–C and C–O Bond Formation between Phenols and Allylic Acetates

Vito Vece,<sup>[a]</sup> Jérémy Ricci,<sup>[a]</sup> Sophie Poulain-Martini,<sup>[a]</sup> Paola Nava,<sup>[b]</sup> Yannick Carissan,<sup>[b]</sup> Stéphane Humbel,<sup>[b]</sup> and Elisabet Duñach\*<sup>[a]</sup>

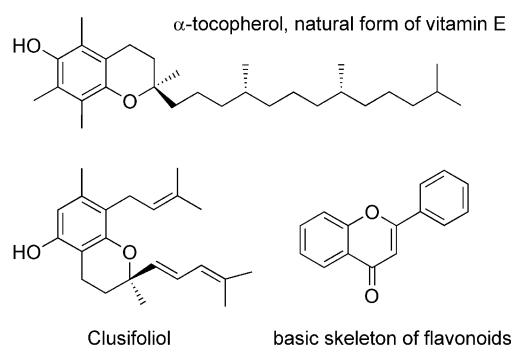
**Keywords:** Indium / Lewis acids / Allylation / Oxygen heterocycles / Tandem reactions

Indium triflate catalysed tandem allylation–intramolecular hydroalkoxylation was efficiently carried out by using 1 mol-% of the catalyst under mild conditions to afford the dihy-

drobenzopyran ring system (chroman-type structure) in good yields. Kinetic, mechanistic and theoretical studies are also presented.

## Introduction

Oxygen-containing heterocyclic compounds are found in many natural and biologically active materials.<sup>[1]</sup> In particular, chroman-type structures constitute a class of highly interesting compounds (Scheme 1) including, for example, vitamin E ( $\alpha$ -tocopherol), the biologically most relevant fat-soluble antioxidant,<sup>[2]</sup> dihydrobenzopyran-derived Clusifoliol, an antitumour agent,<sup>[3]</sup> and flavonoids, polyphenolic compounds ubiquitously found in plants with effects on cancer chemoprevention and chemotherapy.<sup>[4]</sup>



Scheme 1. Examples of biologically active chroman derivatives.

Conventional routes to the chroman framework generally require more than stoichiometric amounts of promoters. The Claisen rearrangement was first reported for the preparation of benzopyrans, involving the reaction of

phenol derivatives and 1,3-dienes at high temperatures.<sup>[5]</sup> Under promotion by a Brønsted or Lewis acid, phenolic compounds may react with isoprene or other 1,3-dienes under homogeneous<sup>[6]</sup> or heterogeneous<sup>[7]</sup> conditions to give directly the corresponding heterocycles. The synthesis of dihydrobenzopyrans from allylic alcohols or derivatives under stoichiometric Brønsted<sup>[8]</sup> or Lewis acid conditions has also been described.<sup>[9]</sup>

Catalytic systems for the preparation of benzopyran structures from phenols and allylic or 1,3-diene derivatives have been reported and include transition-metal catalysis,<sup>[10]</sup> protic catalysis<sup>[11]</sup> and Sc(OTf)<sub>3</sub><sup>[12]</sup> (10 mol-%) catalysis in reactions involving coupling with 1,3-dienes.

The catalytic use of triflate or triflimide salts as Lewis acids for the tandem aryl allylation–cyclisation sequence with allylic acetates has not been extensively explored.<sup>[13]</sup> The development of more efficient catalysts and catalytic methods constitutes an interesting challenge. We report here that In(OTf)<sub>3</sub> is an efficient catalyst for the tandem coupling of phenol derivatives with allylic acetates for the direct synthesis of dihydrobenzopyran structures. Coupling occurs under mild conditions with only 1 mol-% of the catalyst. We also present some insight into the mechanism of this reaction.

## Results and Discussion

### Catalyst Screening

The reactivity of a series of metallic triflates (TfO<sup>-</sup>) and triflimides (Tf<sub>2</sub>N<sup>-</sup>) in the Friedel–Crafts reaction was first examined by using a model system involving phenol (**1a**) and prenyl acetate (**2a**) [Equation (1)]. The reactions were performed with a **1a/2a** ratio of 10:1 in the presence of 1 mol-% of the catalyst in dichloromethane at room temperature. Zn(NTf<sub>2</sub>)<sub>2</sub>, recently reported for the allylation of aryl derivatives with allylic acetates,<sup>[14]</sup> was inefficient for

[a] Laboratoire de Chimie des Molécules Bioactives et des Arômes, Université de Nice-Sophia Antipolis, CNRS, UMR 6001, Institut de Chimie de Nice, Parc Valrose, 06108 Nice Cedex 2, France  
 Fax: +33-4-92-07-61-51  
 E-mail: dunach@unice.fr

[b] UPCAM iSM2 Service D42, UMR 6263, Université Paul Cézanne, 13397 Marseille cedex 20, France

Supporting information for this article is available on the WWW under <http://dx.doi.org/10.1002/ejoc.201000738>.

the tandem allylation–cyclisation reaction starting from phenol (Table 1, Entry 1).  $\text{Zn}(\text{OTf})_2$  as well as  $\text{Ni}(\text{OTf})_2$  and  $\text{Ni}(\text{NTf}_2)_2$  also showed poor catalytic activities (Table 1, Entries 2–4). Good coupling results were obtained at 25 °C with  $\text{In}(\text{OTf})_3$  (Table 1, Entry 5). Cyclised product **3aa** and *para*-allylated noncyclised **4aa** were obtained in a combined GC yield of 81% in a 4.7:1 ratio. *ortho*-Allylated derivative **5aa** was not observed in the final reaction mixture. The reaction was less efficient at 40 °C, with a combined yield of **3aa/4aa** of 45% due to partial polymerisation (Table 1, Entry 6). Catalysis by  $\text{In}(\text{NTf}_2)_3$  led to **3aa/4aa** in 66% yield in a 2.4:1 relative ratio (Table 1, Entry 7). Although the selectivity towards chroman structure **3aa** decreased, the use of TfOH or  $\text{Tf}_2\text{NH}$  as catalysts allowed the allylation of **1a** in yields of 75–76% in protic superacid medium, whereas 81% yield was obtained with  $\text{In}(\text{OTf})_3$  (Table 1, Entries 8 and 9). Moreover, controlling the concentration of acid is crucial to avoid substrate polymerisation.  $\text{In}(\text{OTf})_3$  gives better selectivity than TfOH towards chroman structure **3aa**.  $\text{In}(\text{OTf})_3$  was preferred to TfOH as the catalyst in this study because polymerisation of **2a** occurs in strong protic acidic medium.

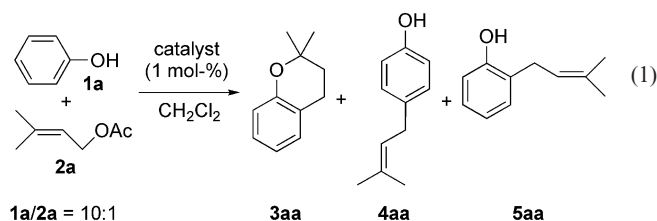


Table 1. Influence of the catalytic system (1 mol-%) in tandem allylation–cyclisation reactions of **1a** with **2a** (**1a/2a** = 10:1,  $\text{CH}_2\text{Cl}_2$ ).

Entry	Catalyst	<i>T</i> [°C]	<i>t</i> [h]	% Yield of <b>3aa</b> + <b>4aa</b> + <b>5aa</b> <sup>[a]</sup>	Ratio <b>3aa/4aa/5aa</b> <sup>[a]</sup>
1	$\text{Zn}(\text{NTf}_2)_2$	25	24	5	1:2:2
2	$\text{Zn}(\text{OTf})_2$	25	24	25	1:11:13
3	$\text{Ni}(\text{OTf})_2$	25	24	4	1:2:1
4	$\text{Ni}(\text{NTf}_2)_2$	25	24	5	1:2:2
5	$\text{In}(\text{OTf})_3$	25	2	81	4.7:1:–
6	$\text{In}(\text{OTf})_3$	40	1	45	4.5:1:–
7	$\text{In}(\text{NTf}_2)_3$	25	24	66	2.4:1:–
8	TfOH	25	1	75	3:1:–
9	$\text{Tf}_2\text{NH}$	25	1	76	3.1:1:–

[a] Yields and product ratios determined by GC with nonane as internal standard.

In addition to the selectivity towards **3aa** attained for this tandem process with  $\text{In}(\text{OTf})_3$ , the reaction operates under mild conditions (room temperature) and was complete in 2 h in the presence of only 1 mol-% of catalyst. Chroman **3aa** could be isolated as a pure compound from the reaction mixture by performing basic aqueous extraction.

### Tandem Allylation–Cyclisation of Phenol Derivatives

With  $\text{In}(\text{OTf})_3$  as the selected catalyst (1 mol-%), the scope of the tandem reaction was extended to include a

variety of phenol derivatives and allylic acetates (Table 2). The formation of substituted chroman structures **3** was first examined with phenol derivatives **1a–h** and acetate **2a**. The reaction proceeded with high regioselectivity in yields ranging from 71 to 95% (Table 2, Entries 1–8). Interestingly, the tandem process was not only efficient and highly selective with activated phenol derivatives, but it was also proceeded with phenol substrates bearing electron-withdrawing substituents (Table 2, Entries 6 and 7).

Whereas **1a** afforded a mixture of **3aa** and **4aa** in 80% yield (Table 2, Entry 1), 3,5-dimethyl-substituted **1b** led to tandem allylation–cyclisation product **3ba** in 95% yield and with an excellent selectivity of 19:1 for **3ba/4ba** (Table 2, Entry 2); less than 5% yield of *para*-allylated phenol **4ba** was obtained from this reaction. For 2,6-dimethyl-substituted **1c** (Table 2, Entry 3), the Friedel–Crafts allylation occurred exclusively at the *para* position, allowing the selective formation of monoallylated isomer **4ca** in 93% yield. This example suggests that the aryl allylation is the first step in this tandem process.

When several 4-substituted phenol derivatives were used, the tandem allylation–cyclisation process occurred with high efficiency (Table 2, Entries 4–7), affording the expected chroman derivatives in 71–94% yields. Coupling of trimethylhydroquinone **1h** to **3ha** was achieved in 86% yield (Table 2, Entry 8). Further reactions were performed with differently substituted allyl acetates (Table 2, Entries 9–13). Chroman structure **3aa** was the major compound formed upon reaction of **1a** with acetate **2b** (Table 2, Entry 9). The outcome of the reaction was the same as that obtained with acetate **2a** (Table 2, Entry 1), suggesting that a carbocationic  $\pi$ -allyl-type common intermediate was generated from both acetates **2a** and **2b**. In the case of disubstituted allylic acetates **2c** and **2d** (Table 2, Entries 10 and 11), a mixture of five- and six-membered ring heterocycles was obtained from the tandem reactions carried out under refluxing conditions in nitromethane. Under the same conditions, methallyl acetate **2e** afforded dihydrobenzofuran **6de** in 41% yield (Table 2, Entry 12). Despite the lower yield due to partial polymerisation, only benzofuran **6de** was obtained, as expected from the double bond substitution. Unsubstituted allyl acetate failed to react. Treatment of acetate **2f** with trimethylhydroquinone **1h** afforded expected vitamin E (**3hf**) in 91% yield as a 1:1 mixture of diastereoisomers (Table 2, Entry 13). Related reactions concerning trimethylhydroquinone coupling have been described under stoichiometric<sup>[15]</sup> and catalytic conditions.<sup>[16]</sup>

### Mechanistic Aspects

The observed reactivity of phenol derivatives with allylic acetates suggests that the formation of dihydrobenzopyrans **3** is facilitated when the aromatic ring is electron rich and also when the allylic acetate bears highly substituted double bonds. The observed order of reactivity of the allylic acetate double bond is: trisubstituted > 1,2-disubstituted > 2,2-disubstituted > monosubstituted. This reactivity suggests a

mechanism involving carbocationic  $\pi$ -allyl-type intermediates formed from the allylic acetates in the presence of the Lewis acid.

Dihydrobenzopyran **3aa** may be obtained from **1a** and **2a** by following two different pathways. The first route involves Friedel–Crafts C-allylation to **4aa** and **5aa** followed by in-

Table 2. In(OTf)<sub>3</sub>-catalysed tandem allylation–cyclisation of phenol derivatives **1** with allylic acetates **2** [1/2 = 10:1, In(OTf)<sub>3</sub> (1 mol-%)].

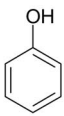
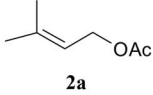
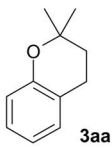
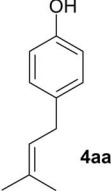
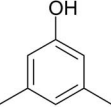
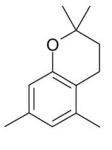
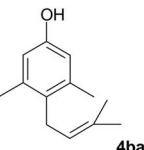
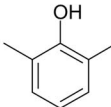
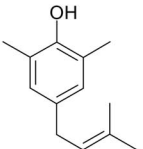
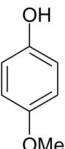
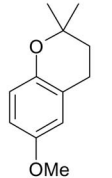
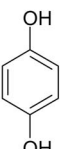
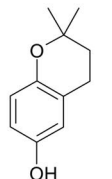
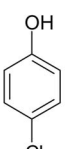
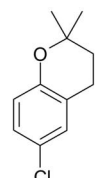
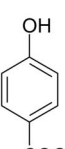
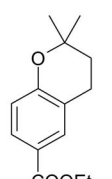
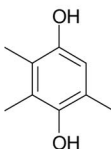
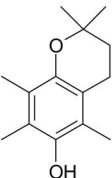
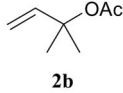
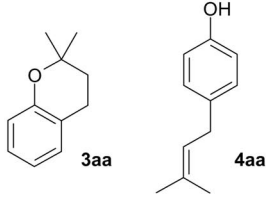
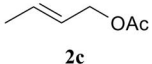
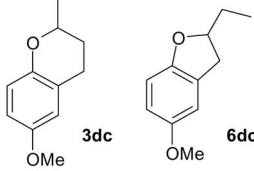
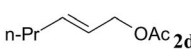
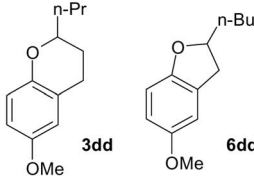
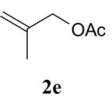
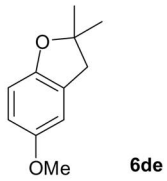
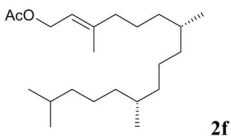
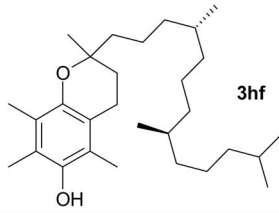
Entry	Phenol compound <b>1a–g</b>	Allylic compound <b>2a–f</b>	Conditions	Products	Isolated yield [%] (isomer ratio <sup>[a]</sup> )
1	 <b>1a</b>	 <b>2a</b>	2 h 25 °C CH <sub>2</sub> Cl <sub>2</sub>	 <b>3aa</b>  <b>4aa</b>	80 ( <b>3aa/4aa</b> = 4.7:1)
2	 <b>1b</b>	<b>2a</b>	4 h 25 °C CH <sub>2</sub> Cl <sub>2</sub>	 <b>3ba</b>  <b>4ba</b>	95 ( <b>3ba/4ba</b> = 19:1)
3	 <b>1c</b>	<b>2a</b>	3 h 40 °C CH <sub>2</sub> Cl <sub>2</sub>	 <b>4ca</b>	93
4	 <b>1d</b>	<b>2a</b>	3 h 25 °C CH <sub>2</sub> Cl <sub>2</sub>	 <b>3da</b>	88
5	 <b>1e</b>	<b>2a</b>	4 h 25 °C CH <sub>2</sub> Cl <sub>2</sub> /THF	 <b>3ea</b>	94
6	 <b>1f</b>	<b>2a</b>	4 h 25 °C CH <sub>2</sub> Cl <sub>2</sub>	 <b>3fa</b>	89
7	 <b>1g</b>	<b>2a</b>	24 h 25 °C CH <sub>2</sub> Cl <sub>2</sub>	 <b>3ga</b>	71
8	 <b>1h</b>	<b>2a</b>	36 h 25 °C CH <sub>3</sub> CN	 <b>3ha</b>	86

Table 2. (Continued)

Entry	Phenol compound <b>1a–g</b>	Allylic compound <b>2a–f</b>	Conditions	Products	Isolated yield [%] (isomer ratio <sup>[a]</sup> )
9	<b>1a</b>		2 h 25 °C CH <sub>2</sub> Cl <sub>2</sub>		80 ( <b>3aa/4aa</b> = 4.7:1)
10	<b>1d</b>		24 h 101 °C CH <sub>3</sub> NO <sub>2</sub>		60 ( <b>3dc/6dc</b> = 2:1)
11 <sup>[b]</sup>	<b>1d</b>		48 h 101 °C CH <sub>3</sub> NO <sub>2</sub>		72 ( <b>3dd/6dd</b> = 2.5:1)
12	<b>1d</b>		20 h 101 °C CH <sub>3</sub> NO <sub>2</sub>		41
13	<b>1h</b>		16 h 40 °C (CH <sub>2</sub> Cl <sub>2</sub> ) <sub>2</sub>		91 <sup>[c]</sup>

[a] Isomer ratios determined by GC and NMR spectroscopy. [b] The catalyst was used in 3 mol-%. [c] Two diastereoisomers, ratio 1:1.

tramolecular cyclisation of *ortho*-allyl phenol **5aa** to **3aa** (Scheme 2, path a). A second sequence for the preparation of **3aa** entails initial formation of allyl aryl ether **9aa** followed by Claisen rearrangement to **10aa** (Scheme 2, path b) and further intramolecular cyclisation to afford **11aa** or **12aa**. From **9aa**, one can also consider a [1,3] sigmatropic rearrangement to **5aa** and further intramolecular cyclisation leading to **3aa**.

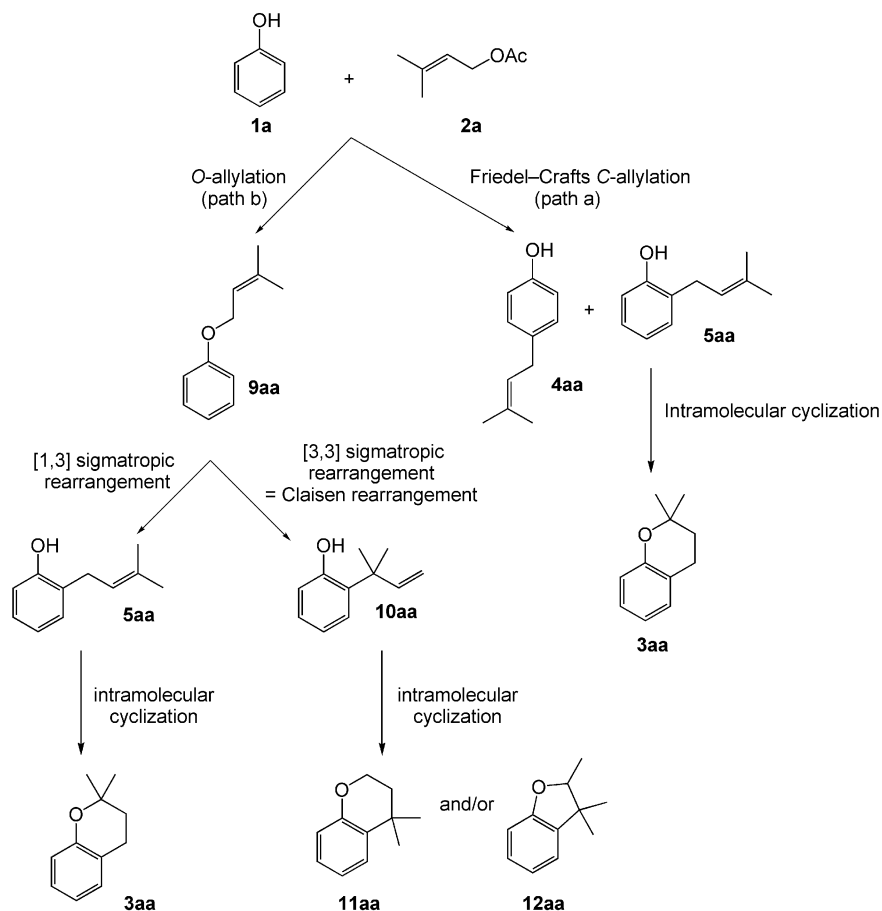
Several Lewis or protic acid catalysed reactions involving the cyclisation of allyl aryl ethers **9** to dihydrobenzofurans **12** or dihydrobenzopyran **3** or **11** have been proposed to involve a [1,3]<sup>[17]</sup> or [3,3] sigmatropic rearrangement.<sup>[18]</sup>

It is worthy to note that intermediates **9aa**, **10aa**, **11aa** and **12aa** were not observed in all In(OTf)<sub>3</sub>-catalysed reactions involving **1a** and **2a**.

We studied the kinetic evolution of the coupling of **1a** and **2a** in a stoichiometric 1:1 ratio, in the presence of

In(OTf)<sub>3</sub> (1 mol-%) in CH<sub>2</sub>Cl<sub>2</sub> at room temperature (Figure 1). The conversion of **2a** was complete within 4 h. After 30 min, *ortho*-C-allylated phenol **5aa** was identified as the major compound of the reaction mixture and its concentration progressively diminished, indicating that **5aa** was an intermediate in this tandem reaction. After 4 h, cyclisation to **3aa** occurred in 33% yield and was accompanied by some *para*-allylation to **4aa** (12%) and some bis(allylation) (20%). The rate of the disappearance of intermediate **5aa** corresponded to that of the appearance of **3aa**, thus arguing in favour of path a in Scheme 2. Ether **9aa** was not observed as an intermediate in this 1:1 reaction.

To gain more insight into the different mechanistic pathways, C- and O-allylated phenols **5aa**, **9aa** and **10aa** were independently prepared and subjected to the In(OTf)<sub>3</sub>-catalysed reaction conditions. Thus, **5aa** was obtained as a by-product in the Mitsunobu reaction of phenol and prenyl



Scheme 2. Alternative mechanistic pathways to chroman structures **3aa**, **11aa** and coumaran derivatives **12aa** from **1a** and **2a**.

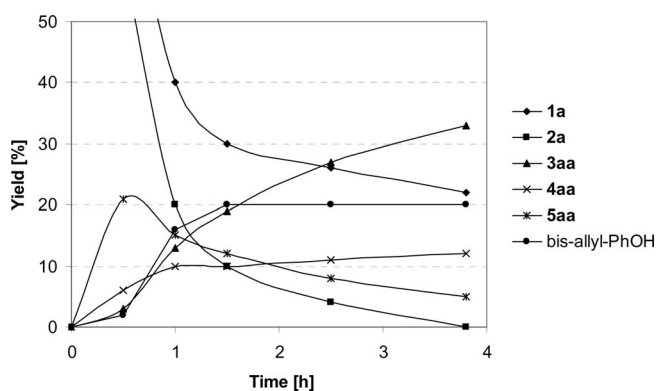


Figure 1. Kinetic evolution of the reaction between **1a** and **2a** [1/2 = 1:1, In(OTf)<sub>3</sub> (1 mol-%), CH<sub>2</sub>Cl<sub>2</sub>, 25 °C].

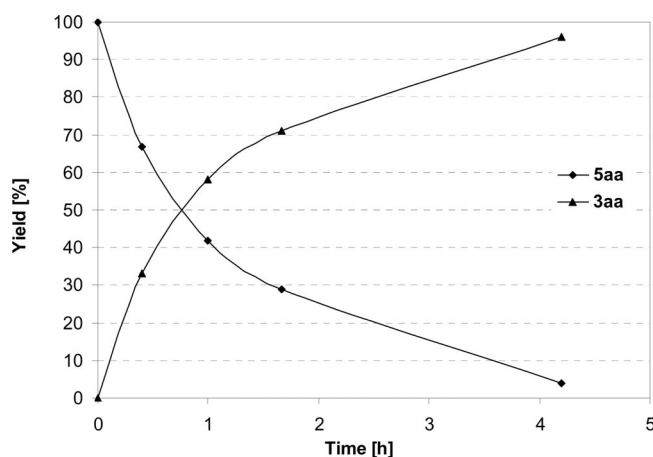


Figure 2. Kinetics of the reaction for the conversion of **5aa** into **3aa** catalysed by In(OTf)<sub>3</sub> (1 mol-%) in CH<sub>2</sub>Cl<sub>2</sub> at 25 °C.

alcohol.<sup>[19]</sup> Ether **9aa** was quantitatively prepared from phenol and prenyl bromide in basic media, and **10aa** was obtained from **9aa** by a Claisen rearrangement at 170 °C.<sup>[20]</sup> The kinetics of the reaction of **5aa** with In(OTf)<sub>3</sub> (1 mol-%) in CH<sub>2</sub>Cl<sub>2</sub> at 25 °C is shown in Figure 2. Cyclic ether **3aa** was the only product formed quantitatively at the same rate as that of the disappearance of **5aa**. This is in favour of **5aa** as an intermediate in the tandem reaction.

When the In(OTf)<sub>3</sub>-catalysed reaction was run with **9aa**, Claisen-type product **10aa** or its corresponding cyclised ether **11aa** (or **12aa**) was not formed. The reaction led directly to **3aa** and **4aa** in 60 and 23% yield, respectively (ratio **3aa/4aa** = 7:3, combined yield of 83%). The formation of **4aa** from **9aa** is indicative of an *O*-allyl cleavage by

$\text{In}(\text{OTf})_3$  presumably by the formation of a  $\pi$ -allyl- $\text{In}^{\text{III}}$  complex in solution as opposed to a regiocontrolled Claisen-type rearrangement. Although **3aa** can be formed from **9aa**, the latter could not be observed in the reaction of **1a** and **2a** under these conditions.

When **10aa** was treated with  $\text{In}(\text{OTf})_3$  (1 mol-%) in  $\text{CH}_2\text{Cl}_2$  at 25 °C, no cyclisation occurred, and this is in agreement with the fact that neither **11aa** nor **12aa** could be detected in reactions of **1a** with **2a** under the  $\text{In}^{\text{III}}$ -catalysed conditions.

To obtain further evidence of allylation being the first step of the reaction (Scheme 2, path a), the  $\text{In}(\text{OTf})_3$ -catalysed system was tested by treating anisole with **2a**. The yield of the reaction was of 81% with a *para/ortho* ratio of 3:1.

In the overall tandem allylation–cyclisation process of phenols with allylic acetates, AcOH is formed as a by-product. To examine the possible influence of AcOH, the  $\text{In}(\text{OTf})_3$ -catalysed reaction of **1a** and **2a** [ratio 1:1,  $\text{In}(\text{OTf})_3$  (1 mol-%),  $\text{CH}_2\text{Cl}_2$ , 25 °C] was carried out in the presence of 1 equiv. of added acetic acid with respect to **1a**. The kinetic evolution and the yield indicated that the addition of AcOH had no significant influence on the process. The cyclisation was however inhibited in the presence of a hindered base such as di-*tert*-butylpyridine (1.2 equiv. with respect to **1a**), indicative of the presence of protons or of the participation of proton shifts in the process.

### Theoretical Calculations

The  $\text{In}(\text{OTf})_3$ -catalysed allylation of **1a** and **2a** was modelled by using DFT calculations. In order to reduce computational cost, the  $-\text{CF}_3$  groups were replaced by chlorine atoms<sup>[21]</sup> and the OTf ligands were designated OTCl. The results were obtained from B3LYP/def2-TZVP+ single-point energy calculations held on BP86/def2-SV(P) geometries.<sup>[22–25]</sup> The Turbomole<sup>[26]</sup> package was used throughout

the study. For the sake of simplicity, only relative energies are presented, always relative to the separated fragments. They include zero-point corrections as calculated at the geometry optimisation level. Absolute energies and detailed xyz coordinates are provided in the Supporting Information.

We computed the mechanistic profiles sketched in Scheme 2. Data obtained for Friedel–Crafts C-allylation (path a) are shown in Figure 3 and the results for O-allylation (path b) are reported in Figure 4. In the following, [In] stands for  $\text{In}(\text{OTCl})_3$ , a dash will represent an H-bonding interaction as in **1a**-[In] and a dot describes a metal–ligand interaction as in [In]·**2a**. As an explanation, starting from the separated reactants,  $\text{In}(\text{OTCl})_3 + \mathbf{1a} + \mathbf{2a}$ , the first proposed complex in the allylation mechanism (Figure 3) is **1a**-[In]·**2a**, in which **1a** is H-bonded to a triflate ligand of the catalyst and allyl acetate **2a** is directly bound to the metal. This complex is situated at  $-21.3$  kcal/mol below the separated fragments.

Let us start with the C-allylation mechanism (Figure 3). From complex **1a**-[In]·**2a**, the first transition state (TS) concerns the transfer of the allylic carbocation generated from acetate **2a** to the phenol ring (computed natural bond orbital<sup>[27]</sup> carbocation charge:  $q_{\text{carbocation}} = +1.2$ ). The optimized geometry of TS **A** (Figure 4) shows optimal allyl transfer conditions, both from electronic and steric points of view: the phenol is loosely H-bonded to one of the triflate groups of the catalyst, but it is not coordinated to the In centre; thus, it preserves its nucleophilic property. Distances between the allyl and the acetate or the phenyl ring are rather large ( $C_{\text{allyl}}-\text{O}_{\text{acetate}} 2.48 \text{ \AA}$ ,  $C_{\text{allyl}}-\text{C}_{\text{phenol}} 2.24 \text{ \AA}$ ), so that the carbocation easily slides from the acetate to the phenol. When acetate **2b** is used instead of **2a**, a very similar structure of **A** arises that leads to intermediate **B**. Once the allyl transfer is completed to give **B** (Figure 4), structural rearrangements occur and the acetate coordinates the metal in an  $\eta^2$  fashion (intermediate at  $-27$  kcal/mol). A proton

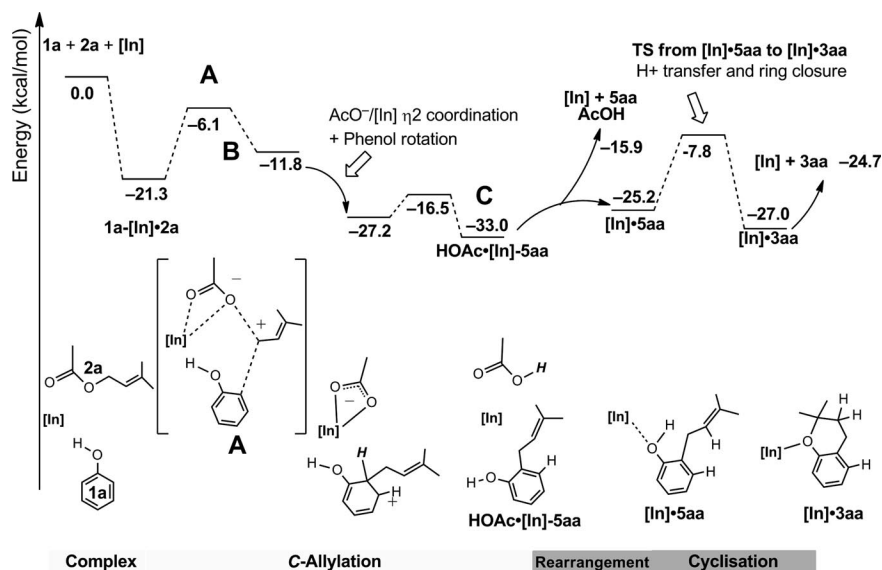


Figure 3. Computed C-allylation from **1a** + **2a** with  $\text{In}(\text{OTf})_3$  to give **5aa**, then cyclisation of **5aa** to **3aa**.

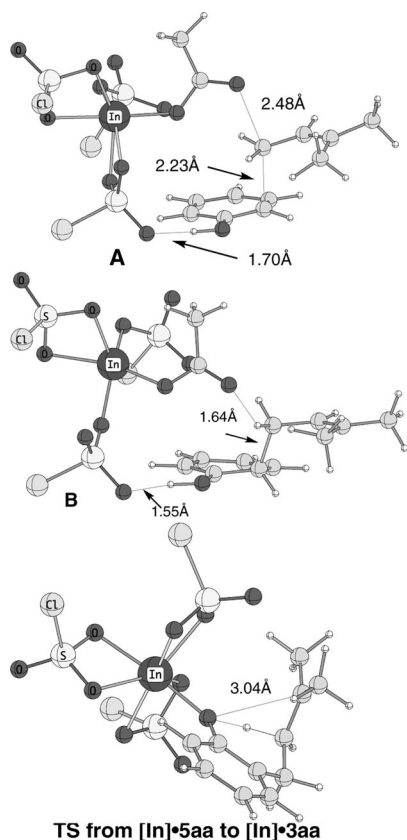


Figure 4. Selected computed structures from Figure 3.

transfer follows to give rise to structure **C** with a barrier of only 11 kcal/mol (TS at  $-16.5$  kcal/mol).

The system affords AcOH and **5aa**, and the In<sup>III</sup> catalyst is released with an overall exothermicity of  $-15.9$  kcal/mol (Figure 3). Alternatively, **5aa** may evolve to **3aa** as the prod-

uct. In this case, **5aa** coordinates the In centre through its OH group. The cyclisation may occur in a two-step process where a proton is first transferred from the phenol to the double bond and then the C–O bond is formed. Nevertheless, calculations suggest that as the proton transfer proceeds in [In]•**5aa**, the cyclisation immediately follows and leads directly to [In]•**3aa**. Product **3aa** and the In<sup>III</sup> catalyst can be released with an overall exothermicity of  $-24.7$  kcal/mol.

Theoretical calculations support the C-allylation mechanism as it does not imply TSs at very high energy. The highest point computed in the energy potential surface corresponds to **A**, at  $-6.1$  kcal/mol. Furthermore, the calculations show the role of the catalyst, which is to promote cleavage of the C–O bond of the acetate (structure **A**) and to promote proton transfer and the ring closure process from [In]•**5aa** to [In]•**3aa** (Figure 3). A 3D view of the TS can be seen in Figure 4. It is shown that the C...O distance is particularly large at the TS, and we conclude that the proton transfer occurs before the C–O bond formation. IRC (intrinsic reaction coordinate) from the TS followed by a careful geometrical optimisation clearly show a one-step mechanism that encompasses both the proton migration and C–O ring closure.

The analysis of the *O*-allylation mechanism (Scheme 2, path b) illustrated in Figure 5 indicates that in this case the phenol coordinates directly to the catalyst and is deprotonated by a triflate ligand (Figure 6). The acetate is also coordinated to the metal centre and is followed by *O*-allylation to give complex [In]•**9aa** (this process is not shown in Figure 4). The energy of the TS for this last step is  $+13.7$  kcal/mol, which is much higher than any point on the computed C-allylation potential energy surface. This result is sufficient to exclude the *O*-allylation mechanism. Nevertheless, it was considered important to study the evolution of the [In]•**9aa** intermediate.

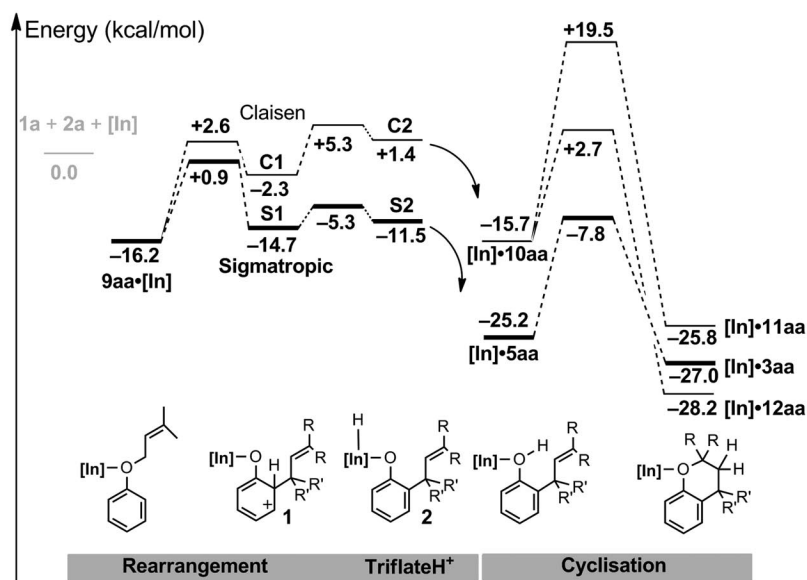


Figure 5. Computed Claisen ( $R = H, R' = Me$ ) and [1,3] sigmatropic ( $R = Me, R' = H$ ) rearrangements from **9aa** to **3aa**, **11aa** and **12aa**. The dashed arrows indicate a proton transfer mediated by a triflate group.

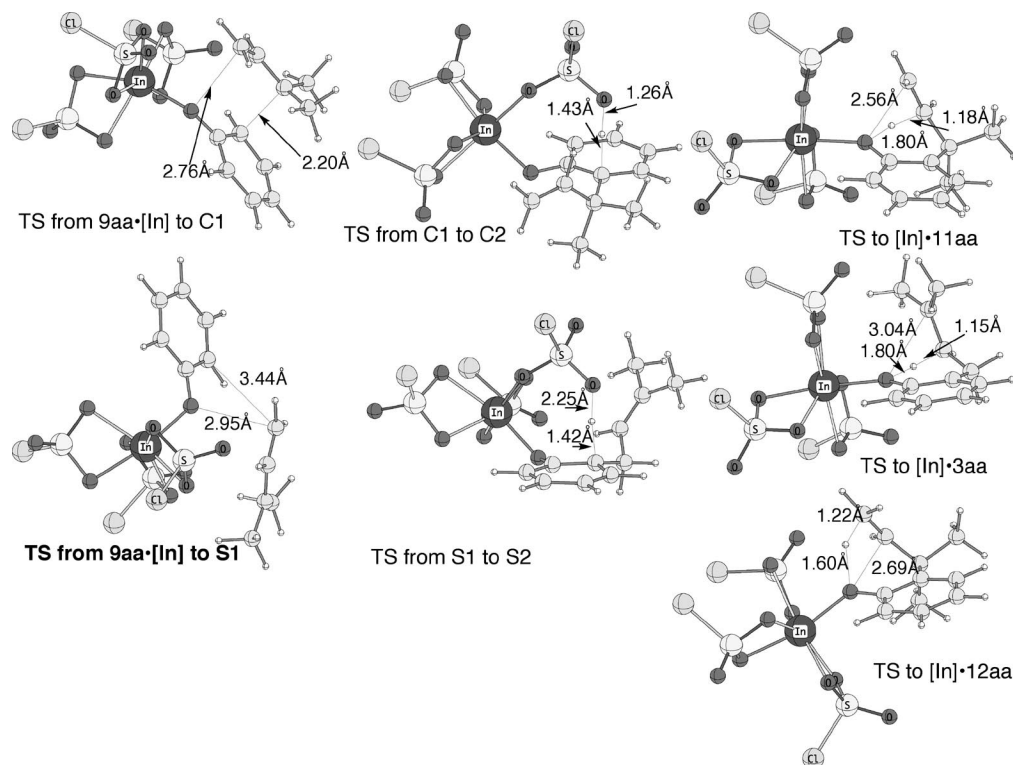


Figure 6. Selected computed structures from Figure 5.

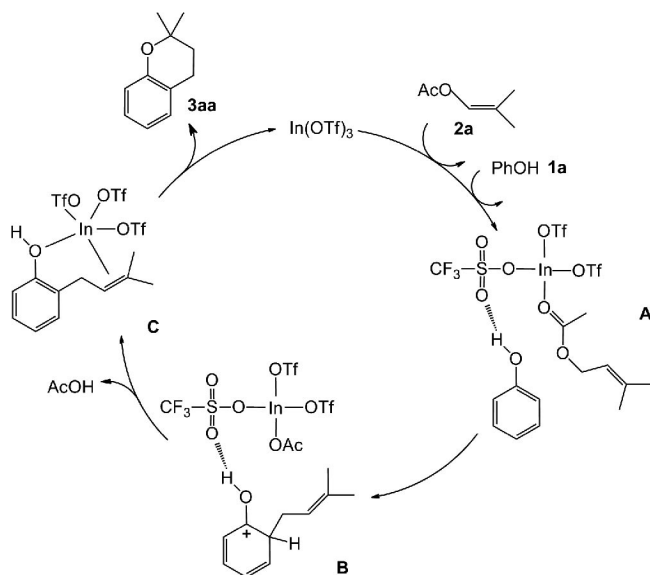
Experiments suggest that **9aa** affords **5aa** after a [1,3] sigmatropic rearrangement rather than a Claisen rearrangement to give **10aa** (Scheme 2). Moreover, whereas **5aa** affords cyclisation product **3aa**, **10aa** fails to react under the same conditions and does not afford **11aa**. Complex  $[\text{In}]\cdot\mathbf{9aa}$  evolves to two Wheland-like intermediates, **S1** and **C1**, according to the [1,3] sigmatropic and Claisen rearrangements, respectively (Figure 5). We noticed that the deprotonation of these intermediates needs **S2** and **C2** triflate-protonated complexes to generate precyclisation species  $[\text{In}]\cdot\mathbf{10aa}$  and  $[\text{In}]\cdot\mathbf{5aa}$ . The direct proton transfer from **S1** (or **C1**) to  $[\text{In}]\cdot\mathbf{5aa}$  (or  $[\text{In}]\cdot\mathbf{10aa}$ ) was also computed and is not favoured, with a TS at 36.5 kcal/mol (or 40 kcal/mol) with respect to the isolated fragments (not shown; see the Supporting Information, Direct proton transfer). Theoretical calculations indicate that the [1,3] sigmatropic rearrangement of  $\mathbf{9aa}\cdot[\text{In}]$  into  $[\text{In}]\cdot\mathbf{5aa}$  is preferred to a Claisen rearrangement that leads to  $[\text{In}]\cdot\mathbf{10aa}$ . The former pathway is overall about 10 kcal/mol lower in energy than the latter (Figure 5) and the energies of the highest TSs for the [1,3] sigmatropic and Claisen rearrangements are 0.9 and 5.3 kcal/mol, respectively.

The further cyclisation step involves a proton transfer from the phenol (Figure 6). An activation energy of 17.4 kcal/mol is required to go from  $[\text{In}]\cdot\mathbf{5aa}$  to  $[\text{In}]\cdot\mathbf{3aa}$ , whereas the activation energy required to go from  $[\text{In}]\cdot\mathbf{10aa}$  to  $[\text{In}]\cdot\mathbf{11aa}$  is significantly higher at 35.3 kcal/mol. This important energy difference is clearly due to the relative stabilities of the primary versus tertiary carbocation in the cor-

responding TSs and explains the observed difference in the experimental reactivity at low temperature. We computationally noted that a five-membered ring cyclisation from  $[\text{In}]\cdot\mathbf{10aa}$  to  $[\text{In}]\cdot\mathbf{12aa}$ , through a relatively stable secondary carbocation, would require 18.5 kcal/mol and would be exothermic by 10 kcal/mol.

### Proposed Catalytic Cycle

Experimental and theoretical results are in agreement with respect to the most favourable pathway of the tandem allylation–cyclisation process. A catalytic cycle is proposed in Scheme 3. The first step concerns the activation of the allylic acetate by  $\text{In}(\text{OTf})_3$ . Coordination of  $\text{In}^{\text{III}}$  to **2a** leads to the formation of a  $\pi$ -allyl derivative,<sup>[28]</sup> which is experimentally justified by the fact that the same products are obtained from isomeric acetates **2a** and **2c** (Table 2, Entries 1 and 9). In the presence of phenol coordinated to  $\text{In}(\text{OTf})_3$  through H-bonding to a triflate group, the Friedel–Crafts allylation takes place preferably at the *ortho* position due to the close space arrangement. After re-aromatisation and elimination of AcOH, **5aa** coordinated to  $\text{In}^{\text{III}}$  undergoes direct intramolecular cyclisation to **3aa**, regenerating the  $\text{In}(\text{OTf})_3$  catalyst. The cyclisation step follows the Markovnikov rules with the attack of the oxygen at the most substituted allylic carbon.



Scheme 3. Proposed catalytic cycle for the tandem Friedel–Crafts allylation–cyclisation process.

## Conclusions

In conclusion, we developed a Lewis acid catalysed tandem allylation–cyclisation process between phenols and allylic acetates, leading mainly to dihydrobenzopyran structures. The process uses only 1 mol-% of  $\text{In}(\text{OTf})_3$  as the catalyst and operates under very mild conditions. Both electron-rich and electron-deficient phenol and allylic acetate derivatives successfully underwent the reaction. This  $\text{In}^{\text{III}}$  catalytic one-pot reaction constitutes an attractive alternative for the construction of O-heterocyclic compounds.

Mechanistic and theoretical studies as well as the observation of the reactivity of several intermediates rule out the classical Claisen rearrangement and suggest a dual role for the Lewis acid catalyst: direct *ortho*-allylation of the phenols followed by intramolecular cyclisation.

## Experimental Section

**General:** All reactions were carried out under a nitrogen atmosphere. Unless otherwise noted, solvents and reagents were obtained from commercial sources and used without further purification. Reactions were monitored by gas chromatography (HP 6890N, equipped with a capillary column VF-1MS, polydimethylsiloxane, 30 m long, internal diameter 0.25 mm, film thickness 0.25  $\mu\text{m}$ , coupled with a FID) and by thin-layer chromatography on plates coated with 0.25 mm silica gel 60  $\text{F}_{254}$  (Merck) with UV light and aqueous potassium permanganate–sodium hydrogen carbonate as visualizing agents. Merck silica gel 60 (0.040–0.063 and 0.063–0.200 mm particle sizes) was used for column chromatography. Flash column chromatography was performed using silica gel (40–63  $\mu\text{m}$ , VWR). NMR spectra were recorded at 200 MHz with a Bruker AC 200 FT spectrometer at room temperature with TMS as an internal standard. Mass spectra were obtained with a mass detector Agilent 5973N coupled to a gas chromatograph Agilent 6890L by performing electron ionisation at 70 eV.

**General Procedure for the Cyclisation of Phenol Derivatives:** Phenol derivatives **1a–h** (30.0 mmol), acetates **2a–f** (3.0 mmol) and  $\text{In}(\text{OTf})_3$  ( $3.10^{-2}$  mmol) were stirred in  $\text{CH}_2\text{Cl}_2$  (1,2-dichloroethane or  $\text{CH}_3\text{NO}_2$ , 15 mL) at 25 °C (or heated at the reported temperature) for 2–48 h. At the end of reaction, the crude mixture was added to aqueous 1 M NaOH (30 mL). The aqueous layer was extracted with  $\text{Et}_2\text{O}$  ( $3 \times 15$  mL). The combined organic layers were washed with aqueous 1 M NaOH ( $3 \times 30$  mL), 1 M HCl ( $3 \times 30$  mL) and saturated aqueous solution of NaCl (30 mL), dried with magnesium sulfate and concentrated under reduced pressure. Final products were purified by basic extraction or by column chromatography on silica gel ( $\text{Et}_2\text{O}$  and/or petroleum ether and/or AcOEt).

The prepared products are known compounds, for details see: 2,2-dimethylchroman (**3aa**),<sup>[29]</sup> 2,2,5,7-tetramethylchroman (**3ba**),<sup>[17a]</sup> 2,6-dimethyl-4-(3-methylbut-2-enyl)phenol (**4ca**),<sup>[30]</sup> 6-methoxy-2,2-dimethylchroman (**3da**),<sup>[31]</sup> 2,2-dimethylchroman-6-ol (**3ea**),<sup>[32]</sup> 6-chloro-2,2-dimethylchroman (**3fa**),<sup>[33]</sup> ethyl 2,2-dimethylchroman-6-carboxylate (**3ga**),<sup>[34]</sup> 6-hydroxy-2,2,5,7,8-pentamethylchroman (**3ha**),<sup>[35]</sup> 6-methoxy-2-methylchroman (**3dc**),<sup>[31]</sup> 5-methoxy-2,2-dimethylcoumaran (**6de**),<sup>[36]</sup> 2,5,7,8-tetramethyl-2-[4(*R*),8(*R*),12-trimethyltridecyl]chroman-6-ol (**3hf**).<sup>[37]</sup> Detailed procedures and spectroscopic data are given in the Supporting Information.

**Supporting Information** (see footnote on the first page of this article): Spectral data for compounds **3**, **4** and **6**; theoretical data for the calculations of Figures 3 and 5.

## Acknowledgments

We thank the French Agence National de la Recherche for financial support of the project Casal (ANR-07-CP2D-04-01).

- [1] H. C. Shen, *Tetrahedron* **2009**, *65*, 3931–3952.
- [2] C. K. Chow, *Curr. Chem. Biol.* **2009**, *3*, 197–202.
- [3] T. Tanaka, F. Asai, M. Iinuma, *Phytochemistry* **1998**, *49*, 229–232.
- [4] E. Middleton Jr., C. Kandaswami, T. C. Theoharides, *Pharmacol. Rev.* **2000**, *52*, 673–751.
- [5] L. Claisen, *Ber. Dtsch. Chem. Ges. B* **1921**, *54B*, 200–203.
- [6] a) V. K. Ahluwalia, K. K. Arora, *Tetrahedron* **1981**, *37*, 1437–1439; b) J. A. M. Laan, F. L. L. Giesen, J. P. Ward, *Chem. Ind.* **1989**, 354–355; c) M. Matsui, H. Yamamoto, *Bull. Chem. Soc. Jpn.* **1995**, *68*, 2657–2661; d) T. Narendar, K. Papi Reddy, Shweta, *Synth. Commun.* **2009**, *39*, 384–394; e) L. Bolzoni, G. Casiraghi, G. Casnati, G. Sartori, *Angew. Chem.* **1978**, *90*, 727–728.
- [7] a) G. P. Kalena, A. Jain, A. Banerji, *Molecules* **1997**, *2*, 100–105; b) F. Bigi, S. Carloni, R. Maggi, C. Muchetti, M. Rastelli, G. Sartori, *Synthesis* **1998**, 301–304.
- [8] a) F. M. D. Ismail, M. J. Hilton, M. Stefinovic, *Tetrahedron Lett.* **1992**, *33*, 3795–3796; b) R. J. Molyneux, L. Jurd, *Tetrahedron* **1970**, *26*, 4743–4751.
- [9] a) P. A. Wehrli, R. I. Fryer, W. Metlesics, *J. Org. Chem.* **1971**, *36*, 2910–2912; b) L. He, S. Galland, C. Dufour, G.-R. Chen, O. Dangles, B. Fenet, J.-P. Praly, *Eur. J. Org. Chem.* **2008**, 1869–1883; c) S. Coman, S. Wuttke, A. Vimont, M. Daturi, E. Kemnitz, *Adv. Synth. Catal.* **2008**, *350*, 2517–2524; d) Y. Tachibana, *Bull. Chem. Soc. Jpn.* **1977**, *50*, 2477–2478; e) Y. Butsugan, H. Tsukamoto, N. Morito, T. Bito, *Chem. Lett.* **1976**, 523–524.
- [10] For examples of transition-metal-mediated synthesis of benzopyrans from phenols, see: a) A. V. Malkov, S. L. Davis, I. R. Baxendale, W. L. Mitchell, P. Kocovsky, *J. Org. Chem.* **1999**, *64*, 2751–2764; b) T. Ohta, Y. Kataoka, A. Miyoshi, Y. Oe, I. Furukawa, Y. Ito, *J. Organomet. Chem.* **2007**, *692*, 671–677; c) V. De Felice, A. De Renzi, M. Funicello, A. Panunzi, A. Saporito, *Gazz. Chim. Ital.* **1985**, *115*, 13–15; d) S. W. Youn, J. I.

- Eom, *J. Org. Chem.* **2006**, *71*, 6705–6707; e) R.-V. Nguyen, X. Yao, C.-J. Li, *Org. Lett.* **2006**, *8*, 2397–2399; f) L. A. Adrio, K. K. Hii, *Chem. Commun.* **2008**, 2325–2327; g) A. Malkov, P. Kocovsky, *Collect. Czech. Chem. Commun.* **2001**, *66*, 1257–1268.
- [11] Y. Ishino, M. Mihara, N. Hayakawa, T. Miyata, Y. Kaneko, T. Miyata, *Synth. Commun.* **2001**, *31*, 439–448.
- [12] S. W. Youn, *Synlett* **2007**, 3050–3054.
- [13] a) W. Bonrath, Y. Foricher, T. Netscher, A. Wildermann (DSM IP Assets B. V.), WO 2005054223, **2005**; b) W. Bonrath, L. Giraudi (DSM IP Assets B. V.), WO 2005005407, **2005**; c) W. Bonrath, C. Dittel, T. Netscher, T. Pabst, L. Giraudi (DSM IP Assets B. V.), WO 2004063182, **2004**.
- [14] J. Ricci, S. Poulain-Martini, E. Duñach, *C. R. Acad. Sci. II C* **2009**, *12*, 916–921.
- [15] For examples of vitamin E synthesis under stoichiometric conditions, see ref.<sup>[6c,7b,8a,9a–9d]</sup>
- [16] For examples of vitamin E synthesis under catalytic conditions, see: a) T. Ichikawa, T. Kato, *Bull. Chem. Soc. Jpn.* **1968**, *41*, 1224–1228; b) M. Matsui, H. Yamamoto, *Bull. Chem. Soc. Jpn.* **1995**, *68*, 2663–2668; c) H. Bienayme, J. E. Ancel, P. Meilland, J. P. Simonato, *Tetrahedron Lett.* **2000**, *41*, 3339–3343; d) L. Tietze, K. Sommer, J. Zingrebe, F. Stecker, *Angew. Chem. Int. Ed.* **2005**, *44*, 257–259; e) M. Matsui, N. Karibe, K. Hayashi, H. Yamamoto, *Bull. Chem. Soc. Jpn.* **1995**, *68*, 3569–3571; f) L. Giraudi, W. Bonrath (DSM IP Assets B. V.), US 2005038269, **2005**.
- [17] a) W. Dauben, J. Cogen, V. Behar, *Tetrahedron Lett.* **1990**, *31*, 3241–3244; b) T. Ollevier, T. Mwene-Mbeja, *Synthesis* **2006**, 3963–3966; c) A. Bernard, M. Cocco, V. Onnis, P. Pier, *Synthesis* **1998**, 256–258.
- [18] a) L. Harwood, *J. Chem. Soc., Chem. Commun.* **1983**, 530–532; b) F. Zulfiqar, T. Kitazume, *Green Chem.* **2000**, *2*, 296–297; c) V. Grant, B. Liu, *Tetrahedron Lett.* **2005**, *46*, 1237–1239; d) Y. Ito, R. Kato, K. Hamashima, Y. Kataoka, Y. Oe, T. Ohta, I. Furukawa, *J. Organomet. Chem.* **2007**, *692*, 691–697; e) N. Reich, C. G. Yang, Z. Shi, C. He, *Synlett* **2006**, 1278–1280; f) K. Kim, H. Kim, E. Ryu, *Heterocycles* **1993**, *36*, 497–505.
- [19] S. Gester, P. Metz, O. Zierau, G. Vollmer, *Tetrahedron* **2001**, *57*, 1015–1018.
- [20] A. Broom, D. Bartholomew, *J. Org. Chem.* **1976**, *41*, 3027–3030.
- [21] P. Nava, Y. Carissan, S. Humbel, *Phys. Chem. Chem. Phys.* **2009**, *11*, 7130–7136.
- [22] a) F. Weigend, R. Ahlrichs, *Phys. Chem. Chem. Phys.* **2005**, *7*, 3297–3305; b) F. Weigend, *Phys. Chem. Chem. Phys.* **2006**, *8*, 1057–1065; c) B. Metz, H. Stoll, M. Dolg, *J. Chem. Phys.* **2000**, *113*, 2563–2569.
- [23] Diffuse functions were added to Cl and O atoms with exponents as in ref.<sup>[20]</sup>
- [24] a) A. D. Becke, *Phys. Rev. A* **1988**, *38*, 3098–3100; b) J. P. Perdew, *Phys. Rev. B* **1986**, *33*, 8822–8824.
- [25] a) S. H. Vosko, L. Wilk, M. Nusair, *Can. J. Phys.* **1980**, *58*, 1200–1211; b) C. Lee, W. Yang, R. G. Parr, *Phys. Rev. B* **1988**, *37*, 785–789; c) A. D. Becke, *J. Chem. Phys.* **1993**, *98*, 5648–5652.
- [26] a) R. Ahlrichs, M. Baer, M. Haeser, H. Horn, C. Koelmel, *Chem. Phys. Lett.* **1989**, *162*, 165–169; b) O. Treutler, R. Ahlrichs, *J. Chem. Phys.* **1995**, *102*, 346–354; c) K. Eichkorn, O. Treutler, H. Oehm, M. Haeser, R. Ahlrichs, *Chem. Phys. Lett.* **1995**, *242*, 652–660; d) P. Deglmann, K. May, F. Furche, R. Ahlrichs, *Chem. Phys. Lett.* **2004**, *384*, 103–107; e) P. Deglmann, F. Furche, R. Ahlrichs, *Chem. Phys. Lett.* **2002**, *362*, 511–518.
- [27] A. E. Reed, R. B. Weinstock, F. Weinhold, *J. Chem. Phys.* **1985**, *83*, 735–746.
- [28] In the calculation, the  $\pi$ -allyl corresponds to TS A situated at –6.1 kcal/mol (Figure 3); its structure is displayed in Figure 4.
- [29] M. Fatope, D. Abraham, *J. Med. Chem.* **1987**, *30*, 1973–1977.
- [30] K. C. Dewhirst, F. F. Rust, *J. Org. Chem.* **1963**, *28*, 798–802.
- [31] K. Hata, H. Hamamoto, Y. Shiozaki, S. Caemmerer, Y. Kita, *Tetrahedron* **2007**, *63*, 4052–4060.
- [32] R. Cichewicz, V. Kenyon, S. Whitman, N. Morales, J. Arguello, T. Holman, P. Crews, *J. Am. Chem. Soc.* **2004**, *126*, 14910–14920.
- [33] Y. Wang, J. Wu, P. Xia, *Synth. Commun.* **2006**, *36*, 2685–2698.
- [34] M. Teng, T. Duong, A. Johnson, E. Klein, L. Wang, B. Khalifa, R. Chandraratna, *J. Med. Chem.* **1997**, *40*, 2445–2451.
- [35] M. Matsuo, S. Urano, *Tetrahedron* **1976**, *32*, 229–231.
- [36] M. Lafrance, S. Gorelsky, K. Fagnou, *J. Am. Chem. Soc.* **2007**, *129*, 14570–14571.
- [37] L. Tietze, F. Stecker, J. Zingrebe, K. Sommer, *Chem. Eur. J.* **2006**, *12*, 8770–8776.

Received: May 21, 2010

Published Online: September 28, 2010